

Methanofullerenes Used as Electron Acceptors in Polymer Photovoltaic Devices

Liping Zheng, Qingmei Zhou, Xianyu Deng, Min Yuan, Gang Yu,[†] and Yong Cao*

Institute of Polymer Optoelectronic Materials and Devices, South China University of Technology, Key Laboratory of Specially Functional Materials and Advanced Manufacturing Technology, Guangzhou 510640, China

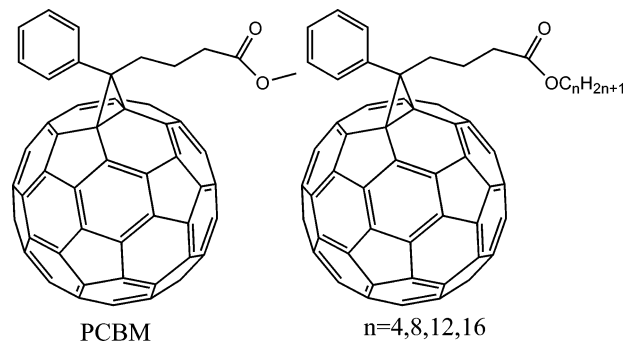
Received: March 12, 2004; In Final Form: May 21, 2004

A series of [6,6]-phenyl C₆₁-butyric acid esters, including methanofullerene [6,6]-phenyl C₆₁-butyric acid methyl ester (PCBM) with different alkyl chain lengths (C₁–C₁₆) was synthesized from the reaction of C₆₀ and alkyl 4-benzoylbutyrate *p*-tosylhydrazone in the presence of sodium methylate. The solubility of C₆₀ derivatives in organic solvents increased with the increase in the length of alkyl substitutions. Photovoltaic cells with these derivatives were fabricated with the structure of ITO/PEDT/MEH–PPV + C₆₀ derivatives/Ba/Al. Device performances with such PCBM analogues were investigated and discussed in terms of Donor/Acceptor (D/A) phase separation and mobility of acceptor phase. The results clearly indicate that both interfacial properties of the two phases (donor and acceptor) and mobility of electrons and holes within corresponding phases play an important role in the efficiencies of PV cells. This study revealed that methanofullerenes [6,6]-phenyl C₆₁-butyric acid butyl ester, PCBB, possesses better photosensitivity than the PCBM, a widely investigated and well-recognized C₆₀ derivative for polymer PV cells. The energy conversion efficiency reaches 2.84% for PCBB under AM1.5 illumination (78.2 mW/cm²), but 2.0% for PCBM fabricated in the same conditions.

I. Introduction

The idea of making thin-film photovoltaic devices from electroactive polymers and organic materials has recently attracted much attention due to the possibility of creating extremely light, cheap, flexible solar cells and photodetectors. Recent research demonstrates that the photoresponse of a homo semiconductor polymer can be further enhanced by being blended with another polymer or an organic molecule with different electronic structures.^{1–4} Photoinduced charge transfer (CT) and subsequent quick charge separation occur in such a blend; that is, the electrons are energetically liable to move into the phase with greater electron affinity (acceptor phase, such as C₆₀ or PCBM), while the photoinduced holes are energetically liable to move into the polymer phase with smaller ionization potential (donor phase, such as poly(2-methoxy-5-(2'-ethylhexoxy)-*p*-phenylene (MEH–PPV)). The photoinduced CT separates electrons and holes and prevents them from early recombination. By carefully controlling the morphology of the D and A phases, one can achieve high interfacial area within a 'bulk D/A heterojunction' material. A bicontinuous network morphology provides pathways with the ability to collect the separated carriers at external electrodes. Thus, phase behavior of D and A components is extremely important to the realization of efficient photovoltaic cells and efficient photodetectors with high carrier collection efficiency.^{5–7} Recently, Sariciftci and co-workers^{8–10} have demonstrated that the power conversion efficiency of bulk-heterojunction plastic solar cells from the blend of a conjugated polymer, poly(2-methoxy-5-(3',7'-dimethyloctyloxy)-1,4-phenylenevinylene) (MDMO–PPV) and PCBM can be raised to 2.5% under AM1.5 irradiation by manipulating the solid-state morphology (nanostructure) of the

SCHEME 1: Molecular Structures of PCBM and C₆₀ Derivatives Used as Acceptor in This Study



blend. They pointed out that the severalfold enhancement in the short-circuit current of photovoltaic devices most possibly originated from enhanced interfacial contacts between the donor and the acceptor. It was also shown that significant improvement in cell efficiency of devices with PCBM as the acceptor phase in comparison with unsubstituted C₆₀ is closely related to the improvement in phase separation of MEH–PPV and PCBM.^{5,7} In the previous paper, we demonstrated that photosensitivity reaches a maximum at a weight ratio of PCBM to MEH–PPV equal to 4.¹³ Device performance deteriorates when the PCBM/MEHPPV ratio is beyond 4. This effect was attributed to reduction of film quality and phase structure of the D/A blend.

Aiming at improving the phase behavior of the polymer PV cells, in this paper we synthesized a series of new C₆₀ derivatives; PCBM analogues [6,6]-phenyl C₆₁-butyric acid ester with alkyl chains length C₄–C₁₆ as acceptor (Scheme 1). Through systematic investigation of chain length influence on the PV cells performance, we found out that, with alkyl length equal to 12 carbon atoms, performance of the PV cells shows only a slight dependence on the length of alkyl chain substitu-

* E-mail: poycao@scut.edu.cn.

[†] Dupont Displays.

tion. Among them, methanofullerenes [6,6]-phenyl C_{61} -butyric acid butyl ester(PCBB) shows better device performance than the PCBM, a widely investigated and the best C_{60} derivative-type acceptor having been reported so far for polymer PV cells. The energy conversion efficiency reaches 2.84% for PCBB under AM1.5 illumination (78.2 mW/cm²), compared with 2.0% for methanofullerenes [6,6]-phenyl C_{61} -butyric acid methyl ester, PCBM, fabricated at the same conditions. Once the alkyl group becomes the $C_{16}H_{33}$, the device performance deteriorates significantly. These results clearly indicate that both the interfacial properties of two phases (donor and acceptor) and the mobility of electrons and holes within corresponding phases play an important role in the efficiency of the PV cells.

II. Experimental Section

Details of synthesis of methanofullerene derivatives (**3a–f**) spectroscopic and analytical data can be found in the Supporting Information.

Cyclic Voltammetry (CV). The electrochemical measurements of the organic molecule were performed in an electrolyte consisting of 0.1 mol/L tetrabutylammonium hexafluorophosphate (TBAPF₆) dissolved in 1,2-dichlorobenzene solution. In each case, a glassy carbon was used as the working electrode, platinum wire was used as a counter electrode, and a saturated calomel electrode was used as a quasi-reference electrode. The absorption spectrum was taken by an HP 8453 spectrophotometer.

The typical device structure used in this study was a sandwich structure with ITO/PEDOT as a hole-collecting electrode and Ba/Al as an electron-collecting electrode. In the structure of the devices, the active layer has a thickness of 100 nm, as determined by surface profilometer (Tencor, ALFA-Step 500). Indium/tin oxide (ITO) was used as the anode and a 50-nm-thick poly (ethylene dioxythiophene)/polystyrenesulfonic acid (PEDT-PSS, Batron-P, Bayer AG) layer was incorporated between the ITO and the active layer to reduce device leakage. Organic molecules as acceptor were dissolved in *p*-xylene or THF solution. MEHPPV was dissolved in a THF/*p*-xylene mixture (2:8) solution. Both solutions were mixed to give the calculated weight ratio of donor material to acceptor material. The blend solution was spincoated onto the top of PEDT-PSS. Finally, 3–5 nm of barium followed by 150-nm-thick Al layers were thermally evaporated onto the top of the photoactive polymer blend. The deposition rates and the thickness of the evaporation layers were monitored by a thickness/rate meter (Sycon). The deposition rates for barium and aluminum were usually 0.01–0.02 nm/s and 1–2 nm/s, respectively. The crossing area between the cathode and the anode define the sensing area. Unless otherwise specified, an 0.15-cm² active area was typically used in this study. All the fabrication steps except spincasting the PEDT:PSS layer were carried out in a nitrogen glovebox. The IV characteristics in the dark and under illumination were measured with a Keithley 236 source-measure unit. Photocurrent was measured under a solar simulator with AM1.5 illumination (78.2 mW/cm²). The spectral response was measured with a commercial photomodulation spectroscopic setup including a Xenon lamp, an optical chopper, a monochromator, and lock-in amplifier operated by PC computer (Merlin, Oriel). A calibrated Si photodiode was used as a standard in determination of photosensitivity.

III. Results and Discussion

Materials. Synthetic route and abbreviations for C_{60} derivatives are shown in Schemes 1 and S2. The [6,6]-phenyl C_{61} -

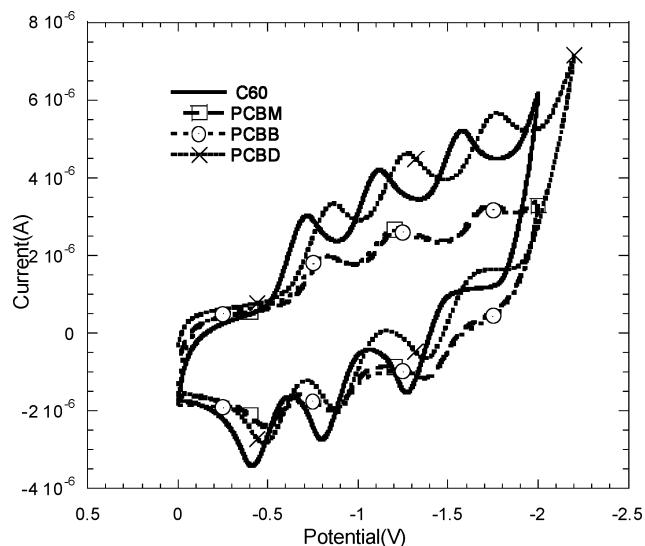


Figure 1. Cyclic Voltammograms of C_{60} derivatives at 50 mv/s in 1,2-dichlorobenzene containing 0.1M (n-Bu)₄NPF₆.

butyric acid esters were synthesized according to Scheme S2 by the diazomethane route reported previously by Hummelen et al.¹¹ All the synthesized fullerene derivatives have been refluxed in 1,2-dichlorobenzene for more than 8 h. The signals for the fullerene-*sp*² carbons in ¹³C NMR spectrum indicate C₅-symmetry. The UV–vis absorbed at 700 nm specific to [6,6] addition in C_{60} . Matrix-assisted laser desorption ionization time-of-flight mass spectrometry (MALDI-TOF-MS) gave the M^- , according to the calculated value of m/z of all the synthesized C_{60} derivatives. The FTIR spectrum showed absorption features at 521 cm⁻¹, indicative of the fullerene core. The synthesized compounds' full and abbreviated names are listed below:

- 3a:** [6,6]-phenyl C_{61} -butyric acid methyl ester, PCBM.
- 3b:** [6,6]-phenyl C_{61} -butyric acid butyl ester, PCBB.
- 3c:** [6,6]-phenyl C_{61} -butyric acid (1-methyl)heptyl ester, PCBMH.
- 3d:** [6,6]-phenyl C_{61} -butyric acid octyl ester, PCBO.
- 3e:** [6,6]-phenyl C_{61} -butyric acid dodecyl ester, PCBDO.
- 3f:** [6,6]-phenyl C_{61} -butyric acid cetyl ester, PCBC.

High molecular weight poly(2-methoxy, 5-(2'-ethylhexyloxy)-1,4-phenylene vinylene) (MEH-PPV) in this study was synthesized according to the process described by Wudl et al.¹²

Electrochemical and Optical Properties of C_{60} Derivatives.

The electrochemical properties of the C_{60} derivatives were studied by cyclic voltammetry at a room temperature in 1,2-dichlorobenzene solution using TBAPF₆ (0.1 M) as the supporting electrolyte. 1,2-dichlorobenzene was used as the solvent for all the C_{60} derivatives that have very good solubility in this solvent. The concentration of C_{60} derivatives (**3a–f**) ranges from 10⁻⁴ to 10⁻³ M. Graphite working electrodes, Pt counter electrodes, and SCE as a reference electrodes were used. All six C_{60} derivatives (**3a–f**) show similar cyclic voltammograms with three quasireversible reduction waves in the potential ranging from 0.0V to -1.8V. To get clear and distinguished curves we choose only three representative curves in Figure 1. More detailed data are listed in Table 1 where E^1_{red} , E^2_{red} , and E^3_{red} reduction potential (defined as the onset of each reduction wave) are listed along with C_{60} and PCBM data obtained in this study and also from the references.⁹ Results in Figure 1 and in Table 1 show that all substituted PCBM have almost identical reduction potential, which indicates that substitution of alkyl chain length in the butyric esters does not affect the reduction potential of C_{60} derivatives.

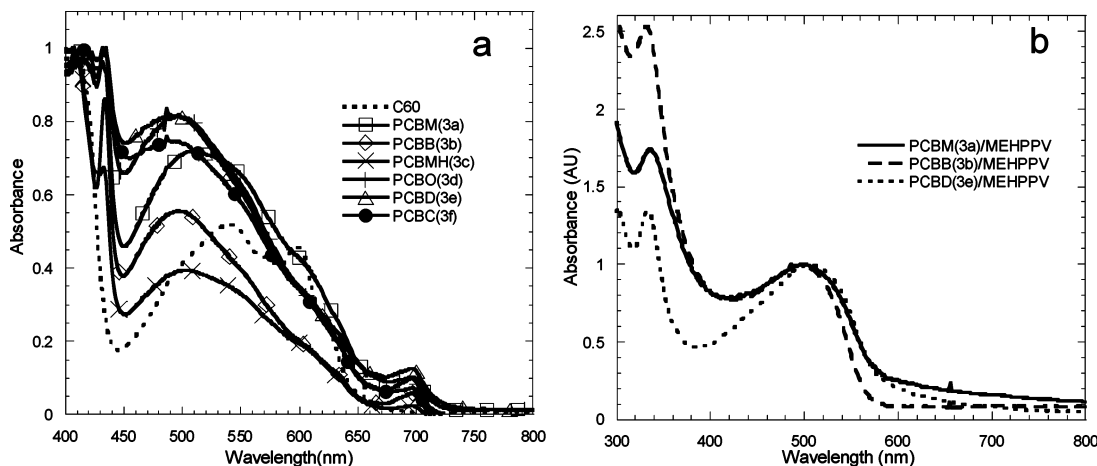


Figure 2. Normalized UV-vis absorption spectra of (a) C₆₀ derivatives in toluene; (b) C₆₀ derivatives/MEHPPV blends (weight ratio equal to 4) solid thin film (film thickness in range 80–110 nm).

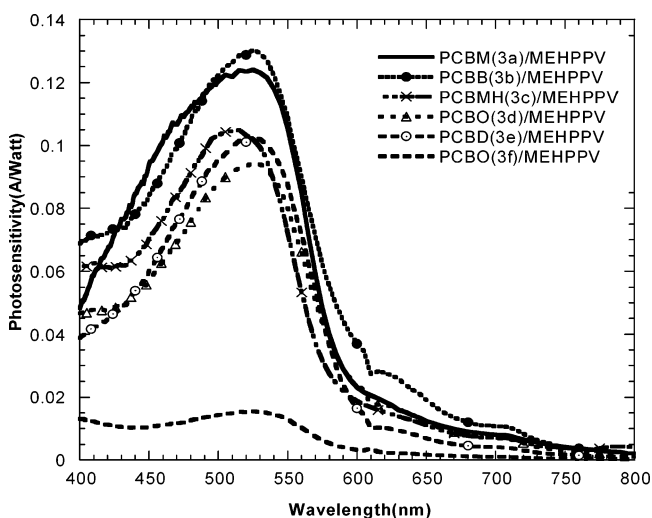


Figure 3. Photosensitivity of devices of ITO/PEDT/MEHPPV+C₆₀ derivatives (1:4 wt ratio)/Ba/Al at 0V bias-voltage.

TABLE 1: Reduction Potentials (V vs SCE) of C₆₀ and Fullerene Derivatives^a

compound	E^1_{red}	E^2_{red}	E^3_{red}
C60	-0.55	-0.95	-1.40
PCBM (3a)	-0.64	-1.05	-1.56
PCBB (3b)	-0.63	-1.05	-1.55
PCBMH (3c)	-0.67	-1.08	-1.59
PCBO (3d)	-0.67	-1.16	-1.69
PCBD (3e)	-0.64	-1.09	-1.57
PCBC (3f)	-0.65	-1.09	-1.62
C60 (ref 11)	-0.60	-1.01	-1.46
PCBM (ref 12)	-0.69	-1.09	-1.57

^a Experimental conditions: 10^{-4} to 10^{-3} mol·L⁻¹ in 1,2-dichlorobenzene solution; TBAPF₆ (0.1M) as supporting electrolyte; Graphite working electrodes, Pt as counter electrodes and SCE as reference electrodes

Absorption spectra obtained from HP 8453 UV-Vis Spectrophotometer are consistent with CV data. Figure 2a shows the UV-visible absorption of **3a–f** in comparison with that of pristine C₆₀ in *p*-xylene solution. It is noted that the absorption profile for the derivatives **3b–f** is very close to that of PCBM (**3a**). These compounds all feature a small peak at 700 nm, specific to [6,6] addition in C₆₀. The main peak at 515 nm in PCBM (**3a**) is slightly blue-shifted to 500 nm in **3b–f**. Meanwhile, the maximum of this peak appears at 540 nm for

pristine C₆₀. From the UV-visible absorption, we conclude that there is no dramatic change in the band structure for compounds **3a–f**.

In summary, CV and absorption spectra data for these C₆₀ derivatives indicate that there should be no dramatic change in energy level alignment upon exchanging each other as the acceptor phase in photovoltaic devices with MEHPPV as donor phase. This characteristic gives us the possibility to investigate phase compatibility without a change in energy level alignment.

Photovoltaic Properties. Photovoltaic cells with a 100-nm thick composite film (weight ratio of methanofullerene:MEHPPV = 4:1 in all cases except indicated otherwise) as the active layer were fabricated by spincoating from chloroform/*p*-xylene (1:1 volume ratio) solution on the top of pre-patterned ITO substrate covered by 100 nm of poly(3,4-ethylene-dioxythiophene):poly(styrene sulfonic acid) (PEDOT: PSS, Baytron P 4083, Bayer AG). A thin layer (3–5 nm) of Ba metal was deposited on the top of the active layer, followed by 200 nm of the Al layer by thermal deposition under vacuum of $(1-2) \times 10^{-4}$ Pa. As we previously reported, a thin layer of Ba inserted between the active layer and the Al cathode improves energy conversion efficiency, serving as an exciton-blocking layer.¹² Salaneck¹⁴ reported that a Ca layer deposited in a low-vacuum evaporating chamber (ca. 1×10^{-4} Pa) was actually partially oxidized. Thus, BaO (or most possibly, nonstoichiometric Ba_{1+x}O_{1-x}) inserted under a negative electrode plays a similar role as an LiF layer on the top of a active layer reported previously by Brabec et al.¹⁵ Device characteristics were measured with a commercial photomodulation spectroscopic setup (Model Merlin, Oriol) including a Xenon lamp, an optical chopper, a monochromator, and lock-in amplifier operated by PC computer. A calibrated Si photodiode was used as a standard in the determination of photosensitivity. Figure 3 compares photosensitivity for devices fabricated from methanofullerenes with different alkyl length as electron acceptors, where the weight ratio of methanofullerenes to MEH-PPV was kept a constant of 4:1. As can be seen from Figure 3, the spectral response is similar for each methanofullerene and is roughly consistent with the absorption curve of the 4:1 blend (Figure 2b). Maximum photosensitivity for all methanofullerene/MEHPPV blends was estimated at around 515 nm.¹³ The magnitude of the photosensitivity of PCBB (**3b**) is slightly larger than that for PCBM (**3a**) blends and then slightly decreases with increasing alkyl chain length.

Photovoltaic characteristics were measured under an AM1.5 solar simulator (78.2 mW/cm²). The current vs voltage was

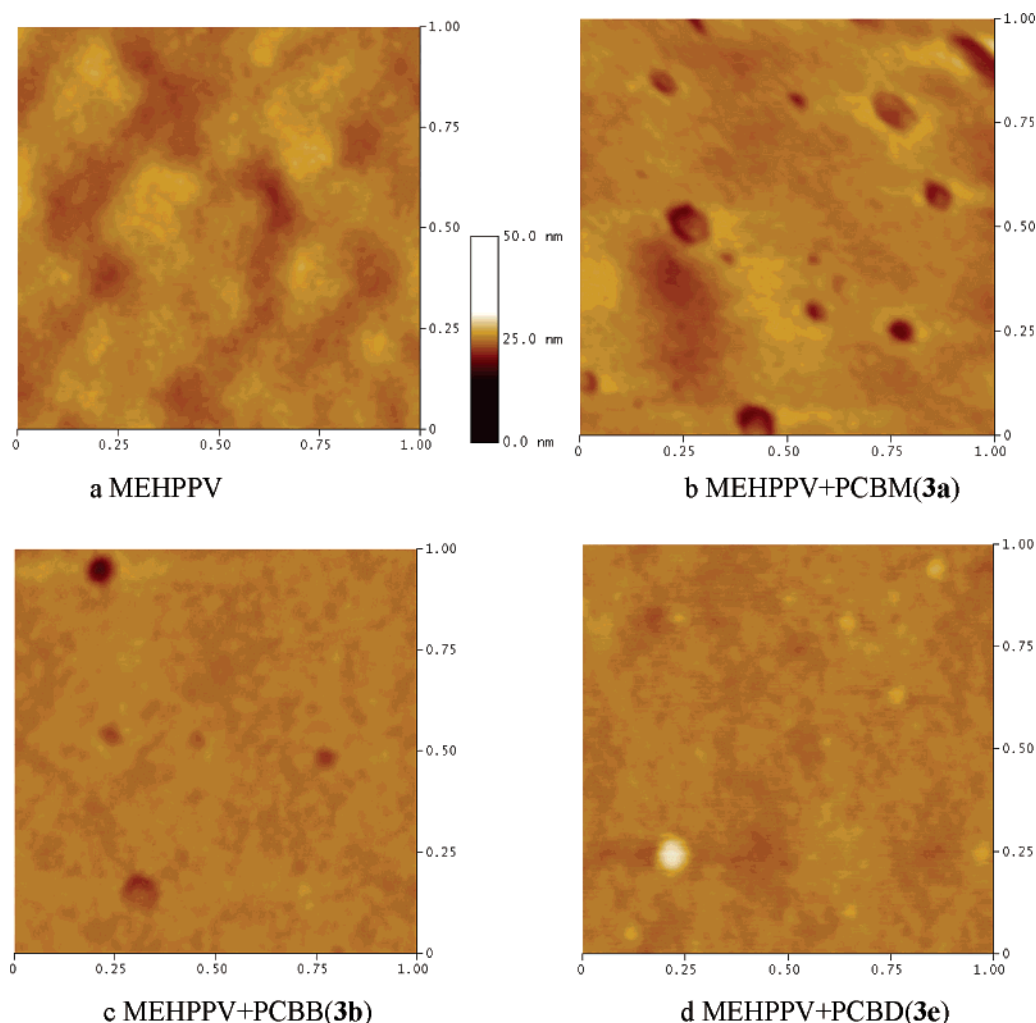


Figure 4. AFM ($1 \times 1 \mu\text{m}^2$) of a 100-nm thick film of MEHPPV and C_{60} derivatives: MEHPPV (4:1) blends spin-coated from toluene solution.

TABLE 2: Photovoltaic Characteristics of Methanofullerenes/MEH-PPV (4:1) Blend-Based Photovoltaic Devices under AM1.5 Illumination ($78.2 \text{ mW}/\text{cm}^2$)

ID	active layer (weight ratio = 4:1)	I_{SC} (mA/cm^2)	V_{OC} (V)	$F.F.$ (%)	ECE under AM1.5	P^*_{smax} (A/W)	λ_{Psmax} (nm)
3a	PCBM/MEHPPV	4.61	0.85	39.9	2.00	0.12	525
3b	PCBB/MEHPPV	5.22	0.85	43.2	2.45	0.13	525
3c	PCBMH/MEHPPV	3.38	0.80	42.3	1.46	0.10	515
3d	PCBO/MEHPPV	3.48	0.80	35.8	1.27	0.09	525
3e	PCBD/MEHPPV	2.86	0.80	35.4	1.04	0.10	525
3f	PCBC/MEHPPV	0.48	0.50	34.0	0.11	0.02	383

measured with a Keithley 236 source-measure unit. The energy conversion efficiency η_e , and fill-factor $F.F.$ were calculated by the following equations:¹⁶

$$\eta_e = F.F. \times I_{\text{sc}} \times V_{\text{oc}}/P_{\text{in}} \quad (1)$$

$$F.F. = I_{\text{m}}V_{\text{m}}/I_{\text{sc}}V_{\text{oc}} \quad (2)$$

where P_{in} is the incident radiation flux, I_{sc} and V_{oc} are the short-circuit current and open-circuit voltage, and I_{m} and V_{m} are the current and voltage for maximum power output.

The results are listed in Table 2. Under the AM1.5 illumination ($78.2 \text{ mW}/\text{cm}^2$), all devices made from **3a–e**, except **3f**, have the same open-circuit voltage of $V_{\text{oc}} = 0.80 \text{ V}$. Generally, a device from the blend with PCBB (**3b**) as acceptor shows better energy conversion efficiency and larger short circuit current than that of a device with PCBM and other methanofullerenes at the same weight ratio of methanofullerene:MEH-

PPV = 4:1 This indicates again that the C4 chain attached to methanofullerene improves its compatibility with the MEHPPV phase without significant decrease in electron mobility in the acceptor phase. We note that the fill factors ($F.F.$) are very close for devices with **3a**, **b**, and **c** but slightly decreases for **3d**, **e**, and **f**. The device from **3f** also shows much lower short-circuit current, which is responsible for the decrease in energy conversion efficiency of factor 10. This indicates that the mobility of substituted methanofullerene with very long alkyl substitution like $\text{C}_{16}\text{H}_{33}$ might be significantly reduced.

Figure 4 compares the AFM height image of pristine MEHPPV and blend films from methanofullerenes and MEHPPV in a weight ratio of 4. It can be seen that, with the increase of alkyl length, the film homogeneity increases. In contrast to the relatively smooth surface of pristine MEHPPV, the blend film of MEHPPV with PCBM (**3a**) shows large numbers of voids in the film, which must be related to incompatibility of

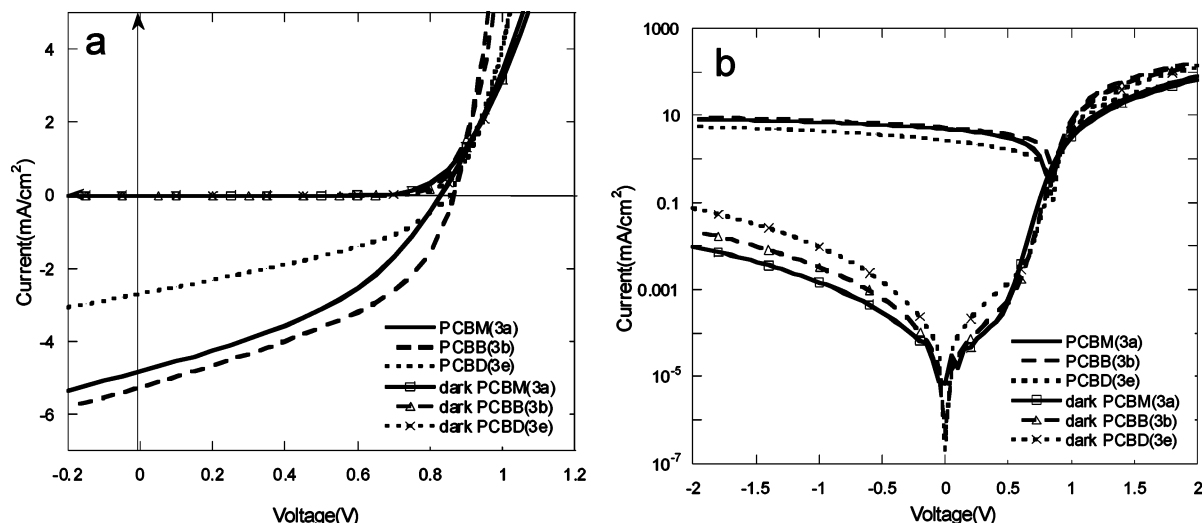


Figure 5. (a) Linear and (b) semilogarithmic plot of the current–voltage characteristics for **3a**, **3b**, and **3e** photovoltaic devices in the dark and under AM 1.5 white-light illumination.

MEHPPV and PCBM during film formation. With the increasing of alkyl length in methanofullerenes (Figure 4b–d), the number of voids decreases remarkably; its depth also decreases. This fact unambiguously indicates that the compatibility and film quality increase with increasing alkyl length. Actually, C_{60} with long alkyl substitution can provide a good quality film of methanofullerenes alone by simple spincoating of the corresponding solution, while PCBM and C_{60} alone cannot form a good film without blending with a polymer host. As a result, we can expect the increase in photosensitivity with the increasing length of alkyl substitutions in the methanofullerenes, if phase compatibility is the only issue. Since no remarkable increase in photosensitivity is observed with increasing the chain length, except C4 substitution, there should be another important factor that lowers the photosensitivity performance. The possible mechanism is that the mobility might decrease with the increase in alkyl substitution, which can separate C_{60} cores and increase barrier height for carrier tunneling between C_{60} cores.

Figure 5 shows the linear (Figure 5a) and semilogarithmic (Figure 5b) plot of the I–V curve of devices from the blend with **3a**, **3b**, and **3e** in the dark and under AM1.5 illumination (78.2 mW/cm^2). The I/V characteristics of the cells prepared from **3a**, **3b**, and **3e** show a good diode behavior with a rectification ratio of ~ 2000 at $\pm 2 \text{ V}$ in the dark. From the semilogarithmic plot of the I–V, it can be clearly seen that not only photo current but also dark current decreases with the increasing length of alkyl substitutions. This fact supports the speculation about the decrease in carrier mobility with increasing alkyl chain length in methanofullerenes.

Further evidence for better compatibility between methanofullerenes of long alkyl substitutions with MEHPPV can be obtained from investigation of device performance as function of blend composition (weight ratio of methanofullerene to MEH–PPV). As we reported previously,¹² the photosensitivity is very sensitive to the weight ratio of PCBM to MEHPPV in the blend film. The maximum photosensitivity for the PCBM/MEHPPV blend is observed when the weight ratio of PCBM/MEHPPV is equal to 4. With the further increase in PCBM ratio photosensitivity decays remarkably. In Table 3 we compare the energy conversion efficiencies (ECE) of devices from the blend of MEHPPV and PCBB (3b) in different weight ratios. The results indicate that the ECE reaches a maximum at a weight ratio of PCBB:MEHPPV = 32:1. At this weight ratio, energy conversion efficiency increases from 2.45% for a 4:1 weight

TABLE 3: Device Performance of PV Cells from Blends of PCBB (3b) and MEH–PPV in Different Weight Ratio

active layer	weight ratio	I_{sc} (mA/cm ²)	V_{oc} (V)	F.F. (%)	ECE (%)
PCBB/MEHPPV	4:1	5.22	0.85	43.2	2.45
PCBB/MEHPPV	8:1	5.28	0.85	45.2	2.60
PCBB/MEHPPV	16:1	5.01	0.85	46.3	2.52
PCBB/MEHPPV	32:1	6.08	0.85	43.0	2.84
PCBB/MEHPPV	64:1	5.03	0.80	42.0	2.16

TABLE 4: Device Performance of PV Cells from Blends of 3f and MEH–PPV in Different Weight Ratio

3f:MEH–PPV weight ratio	I_{sc} (mA/cm ²)	V_{oc} (V)	F.F. (%)	P_s^a (A/W)
18:1	1.1	0.80	40.337	0.05
12:1	1.3	0.75	40.476	0.04
8:1	1.0	0.75	39.038	0.05
4:1	1.8	0.80	37.415	0.06
3:1	1.1	0.75	39.402	0.05
2:1	0.9	0.75	38.549	0.06
1:1	0.8	0.75	39.325	0.04

^a Data at 520 nm.

ratio to 2.84%. The short-circuit current increases slightly from 5.22 to 6.08 mA/cm². Further increasing the PCBB:MEHPPV weight ratio to 64:1 leads to decreasing device performance. Similar results can be obtained for other long-chain alkyl-substituted methanofullerenes. Table 4 shows the device performance when the weight ratio of 3f:MEH–PPV varies from 1:1 to 18:1. We note from the results in Table 4 that all device characteristics are almost constant until a weight ratio of 18:1. Results in Tables 3 and 4 indicate unambiguously the importance of compatibility of the donor and acceptor phases. Longer alkyl chain substitution improves compatibility of donor and acceptor phases. This feature is not only important for device efficiency but also for long-term stability of such devices. The improved compatibility of donor and acceptor phase might prevent self-aggregation of D and A phases in the blend during storage and operation. Corresponding experiments for the comparison of shelf and stress life are in progress.

IV. Conclusions

A series of PCBM analogues was synthesized. Alkyl groups of different lengths were introduced into the tail of the methanofullerenes. The electrochemical and photophysical

properties of the new methanofullerenes were characterized by using CVs and UV–visible spectroscopy. The CVs of all of these methanofullerenes show almost the same quasireversible reduction waves ranging from 0V to $-2.0V$. All the synthesized C₆₀ derivatives exhibit similar absorption spectra. Photovoltaic cells were fabricated from the blend of the obtained methanofullerenes with MEHPPV. With the alkyl length equal to 1–12 carbon atoms, the PV cells show only slight dependence on the length of alkyl chain substitution. The best device performance has been obtained for PCB_B with butyl substitution: the device with $I_{sc} = 6.08$ mA/cm², $V_{oc} = 0.85$, $F.F. = 43.0\%$, and $ECE = 2.84\%$ at PCB_B:MEHPPV weight ratio equal 32:1, but the device with $I_{sc} = 4.61$ mA/cm², $V_{oc} = 0.85$, $F.F. = 39.9$, and $ECE = 2.00\%$ for the best device with PCB_M:MEHPPV = 4:1 under AM1.5 illumination (78.2 mW/cm²). Once the alkyl group reached C₁₆H₃₃, the device performance deteriorated significantly. The results clearly indicate that both interfacial properties of two phases (donor and acceptor) and mobility of electron and holes within corresponding phases (tunneling barrier between C₆₀ cores) are important for the efficiencies of PV cells. To further improve the device performance for such a bulk p–n junction system, it is important to synthesize the acceptor that has high carrier mobility and good compatibility with donor-type conjugated polymer simultaneously.

Acknowledgment. Financial support for this work from the NSFC Project (#50028302) and MOST project (#2002CB613400) is greatly appreciated. We are also grateful to Mr. Ning Bin and Prof. Zhi-Xin Guo of Institute of Chemistry, Chinese Academy of Science, for their help in CV measurement.

Supporting Information Available: Synthetic route, synthesis of methanofullerene derivatives (3a–f) spectroscopic and

analytical data. This material is available free of charge via the Internet at <http://pubs.acs.org>.

References and Notes

- (1) Sariciftci, N. S.; Smilowitz, S. L.; Heeger, A. J.; Wudl, F. *Science* **1992**, *258*, 1474.
- (2) Yu, G.; Pakbaz, K.; Heeger, A. J. *Appl. Phys. Lett.* **1994**, *64*, 3422.
- (3) Yu, G.; Gao, J.; Hummelen, J. C.; Wudl, F.; Heeger, A. J. *Science* **1995**, *270*, 1789.
- (4) Friend, R. H.; Gymer, R. W.; Holmes, A. B.; Burroughes, J. H.; Marks, R. N.; Taliani, C.; Bradley, D. D. C.; Dosantos, D. A.; Bredas, J. L.; Lodlund, M.; Salaneck, W. R. *Nature* **1999**, *397*, 121.
- (5) Yu, G.; Heeger, A. J. *J. Appl. Phys.* **1995**, *78*, 4510.
- (6) Halls, J. J. M.; Walsh, C. A.; Greenham, N. C.; Marseglia, E. A.; Friend, R. H.; Moratti S. C.; Holmes, A. B. *Nature* **1995**, *376*, 498.
- (7) Yu, G.; Gao, J.; Yang, C. Y.; Heeger, A. J. In *Proceedings of SPIE Photodetectors: Materials and Device*; Brown, G. J., Rzeghi, M., Eds.; SPIE-The International Society for Optical Engineering: Bellingham, Washington, 1997; 2999, 306.
- (8) Shaheen, S. E.; Brabec, C. J.; Padinger, F.; Fromherz, T.; Hummelen, J. C.; Sariciftci, N. S. *Appl. Phys. Lett.* **2001**, *78*, 841.
- (9) Brabec, C. J.; Cravino, A.; Meissner, D.; Sariciftci, N. S.; Fromherz, T.; Rispen, M. T.; Sanchez, L.; Hummelen, J. C. *Adv. Funct. Mater.* **2001**, *11*, 374.
- (10) Gebeyehu, D.; Brabec, C. J.; Padinger, F.; Fromherz, T.; Hummelen, J. C.; Badt, D.; Schindler, H.; Sariciftci, N. S. *Synth. Met.* **2001**, *118*, 1.
- (11) Hummelen, J. C.; Knight, B. W.; Peq F. L.; Wudl, F. *J. Org. Chem.* **1995**, *60*, 532.
- (12) Wudl, F.; Khemani, K. C.; Harlev, E.; Ni, Z.; Srdanov, G. *Polym. Mater. Sci. Eng.* **1991**, *64*, 201.
- (13) Deng, X. Y.; Zheng, L. P.; Mo, Y. Q.; Yu, G.; Yang, W.; Weng, W. H.; Cao, Y. *Chin. J. Polym. Sci.* **2001**, *19*, 567.
- (14) Broems, P.; Birgersson, J.; Johansson, N.; Loegdlund, M.; Salaneck, W. R. *Synth. Met.* **1995**, *74*, 1514.
- (15) Brabec, C. J.; Shaheen, S. E.; Winder, C.; Sariciftci, N. S. *Appl. Phys. Lett.* **2002**, *80*, 1288.
- (16) Yu, G.; Srdanov, G.; Wang, H.; Cao, Y.; Heeger, A. J. Organic Photovoltaics. In *Proceedings of SPIE*; SPIE-The International Society for Optical Engineering: Bellingham, Washington, 2001; 4108, 48.